FINITE ELEMENT STUDIES OF THE CANREB ELECTRON GUN FOR A TEST STAND SETUP

M. Hartmann*, F. Ames, J. Cardona, C.R.J. Charles, M. Dehghan, M. Good, S. Ismagilova, O. Kester, A. Kwiatkowski, B. Schultz, TRIUMF, Vancouver, Canada

Abstract

The CANadian Rare isotope facility with Electron Beam ion source (CANREB) is an important component of the Advanced Rare IsotopE Laboratory (ARIEL) at TRIUMF. CANREB will deliver highly charged radioactive ion (HCI) beams for post-acceleration to nuclear physics experiments. Ion beams injected into CANREB are bunched using a radiofrequency quadrupole (RFQ) cooler-buncher and energy adjusted using a pulsed drift tube for injection into an electron beam ion source (EBIS) charge state breeder. Charge breeding occurs by collisions with an electron beam (up to 15 keV, 500 mA) produced by an electron gun. During EBIS commissioning, the electron gun became unstable at currents above 40 mA, with a large fraction of the beam intercepted by the anode. To address this issue, an electron gun with an updated design is planned to be fabricated and installed in CANREB. In order to characterise the new electron gun, a test-stand will be built allowing for systematic testing. This paper describes a full simulation model of the test-stand using Finite Element Analysis (FEA) software TRAK.

INTRODUCTION

The TRIUMF cyclotron delivers a 500 MeV CW (23 MHz) proton beam with currents up to 120 µA to spallation and meson production targets for particle, nuclear, and solid-state physics research [1]. Rare isotope beams (RIBs) are produced by irradiating solid U, Ta, Si, Th, Nb, or C targets with 480 MeV protons at currents up to 100 µA [2]. The resulting ions are extracted at energies up to 60 keV and delivered either to low-energy experimental stations at the ISAC facility or to a multi-stage linac for further acceleration and high-energy experiments. TRIUMF's ARIEL facility [3] will add two new target stations for RIB production as well as integrating the CANadian Rare isotope facility with Electron Beam ion source (CANREB) for charge breeding of ions [2] (Fig. 1). CANREB uses an electron beam ion source (EBIS) to produce highly charged ions (HCI). The EBIS accepts ions with energies up to 14 keV and confines them electrostatically within the center of a split-bore superconducting Helmholtz magnet operating at fields up to 6 T. An electron gun generates an electron beam that is compressed in the trapping region before being collected by an electron collector. During EBIS commisisoning, the electron gun became unstable at currents above 40 mA, with a large fraction of beam intercepted by the anode [2]. To overcome these limitations, an upgraded design is being developed for installation in CANREB. A dedicated test-stand will be constructed to

* mhartmann@triumf.ca

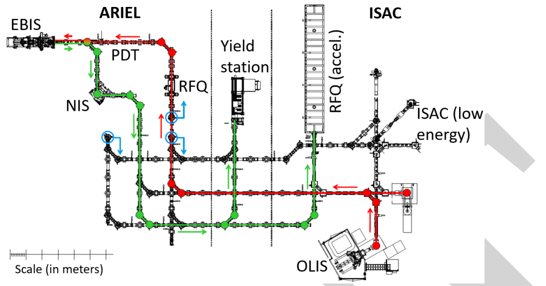

Figure 1: The CANREB facility at ARIEL [4]. Beam is injected from the ISAC RIB targets or the off-line ion source (OLIS) along the red path. The charge-bred beam is extracted via the green path and directed either to the yield station or the ISAC linac. In the future, beams from the ARIEL RIB targets (blue circles) will also be injected into CANREB.

facilitate detailed and reproducible performance studies of the new electron gun. This paper presents a complete simulation model of the test-stand using FEA software TRAK (Field Precision) [5] as well as benchmarking with ion optics code, IGUN [6]. In the following section the electron gun model (design and simulation) is described.

ELECTRON GUN AND TEST-STAND MODEL

Electron Gun Components

Figure. 2 shows an axial cross-section of the new CANREB electron gun. It is a Brillouin-type gun [7] com-

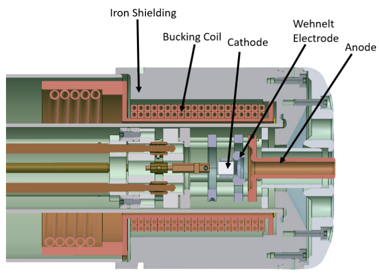

Figure 2: Cross section of the new CANREB electron gun.

prising a 6.35 mm, spherically shaped barium dispenser cathode producing an electron beam of energy up to 15 keV (500 mA). Downstream of the cathode, a high purity copper anode accelerates the emitted electrons. Between the cathode and anode, a focusing electrode (Wehnelt Electrode) shapes the electric field around the cathode, providing efficient control over the electron beam emission [8]. The potential applied to the Wehnelt Electrode can be used to rapidly switch the emission current on and off (a higher negative potential compared to the cathode will suppress the electron beam entirely). To achieve maximum electron-beam compression between the cathode and the trapping region, the fringe magnetic field from the EBIS superconducting magnet must be minimized at the cathode surface. Both passive and active shielding are employed, using a layer of pure ARMCO iron shielding and a 40-turn bucking coil respectively [8].

Test-Stand Design

To validate and characterise the new electron gun, the test-stand must allow electrons to be emitted at the maximum current required for ion charge breeding, exit through the anode, and be compressed by a sufficiently strong magnetic field. It must also provide a means for the electrons to be safely collected and deposited.

Since the test-stand is expected to be separated from the EBIS magnet, an appropriate structure is required to host the electron gun and collection surface. To this end, a custom-designed four-way ConFlat Flange (20 cm diameter) cross is intended to be built. Figure 3 illustrates the set-up. The cross uses two internally attached ConFlat tubes of diameter 11.4 cm, with the left tube attached to the electron gun chamber and the right tube hosting a high-power copper Faraday Cup for collecting electrons and measuring the beam current [1]. A few centimeters upstream of the Faraday Cup, a copper protection collimator and an aluminium plate are fitted to safely collect the beam that does not impinge onto the Faraday Cup and to supress secondary electrons respectively. A vacuum level of 1×10^{-10} Torr is expected inside the cross. Importantly, on the outside of the cross, two flat

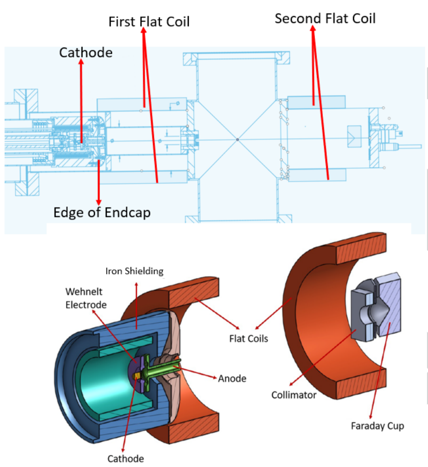

Figure 3: Upper: Test-Stand setup showing custom-designed four-way ConFlat Flange. Lower: 3D rendering showing important components.

coils wound around the tubes are required to produce a sufficiently strong magnetic field for electron beam compression in the region between the exit of the anode and the Faraday Cup. While the first flat coil is placed as close as possible to the gun and is expected to provide the majority of the compression, the second coil provides the final compression to the Faraday Cup collection surface. The mechanical and electrical details of the coils are illustrated in Table 1.

Table 1: Mechanical and electrical parameters for the two test-stand coils.

	First Flat Coil	Second Flat Coil
NI (A-turns)	4000	3000
Turns *N*	120	120
Current *I*	33.3 A	25 A
Wire diameter	6 mm	6 mm
Layers	7	7
Turns/layer	18	18
Coil length	64.7 m	64.7 m
Resistance	0.038 Ω	0.038 Ω
Voltage	1.27 V	0.95 V
Power	42.3 W	23.8 W
Current density	$1.18\ \mathrm{A/mm^2}$	$0.88\ \mathrm{A/mm^2}$

While both coils operate at or below the reference current density of $1\ \mathrm{A/mm^2}$ for air cooling [10], water cooling would become necessary if a higher magnetic field is required for the same geometry.

TRAK Simulation Model

A simulation model of the test-stand was built in TRAK to ensure that its requirements were met. TRAK uses finite element methods to calculate single-particle trajectories in 2D electric and magnetic fields, with support for particle distribution generation and self-consistent space-charge calculations. Figure 4 shows the TRAK geometry generated using variable triangular conformal meshes. A 0.01 cm

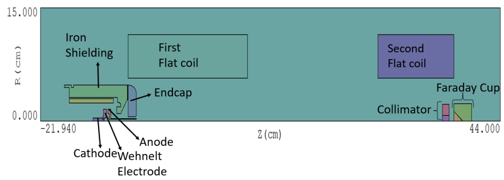

Figure 4: Axisymmetric TRAK geometry of test-stand. The cathode is placed at Z = -12.85 cm and the Faraday Cup is approximately 50 cm from the cathode.

mesh size was used near the electrodes and Faraday Cup to accurately resolve electron emission and collection while maintaining convergence.

ELECTROMAGNETIC FIELDS

In electrostatic simulations, the electric potential is evaluated at mesh nodes, while material properties are assigned to the triangular elements. The space charge limited emission of non-relativisitic electrodes from the cathode surface is described by the Child–Langmuir (CL) law [11]:

$$j_{CL} = \frac{4}{9}\epsilon_0 \left(\frac{2e}{m_e}\right)^{1/2} \frac{V^{3/2}}{d^2} \quad (1)$$

[1] Simulations show that the Faraday Cup reaches a maximum temperature of 313 °C for a 10 keV (100 mA) electron beam with FWHM 6 mm impinging on the inner aperture (1 cm) of the Faraday Cup. The cup is water cooled with an inlet temperature of 20 °C and a flow rate of 3 L/min. Since at this temperature no damage to copper is foreseen and since the same Faraday Cup has been used in previous test-stands at higher power [9], its use for this test-stand is deemed acceptable.

(where j_{CL} is the extracted current density, ε_0 is the vacuum permittivity, e is the elementary charge, m_e is the electron mass, V is the accelerating potential, and d is the distance between anode and cathode). In all simulations a nominal beam of 100 mA and 10 keV is considered. Based on the CL law, a potential difference of approximately 3200 V between the anode and cathode is required to obtain the nominal extracted current, assuming the cathode is held at -1500 V (the maximum power supply for the cathode at CANREB is -3000 V). In order to focus the beam, a slightly lower voltage of -1510 V is applied to the Wehnelt Electrode. The electrostatic solution using these voltages is shown in Fig. 5. The

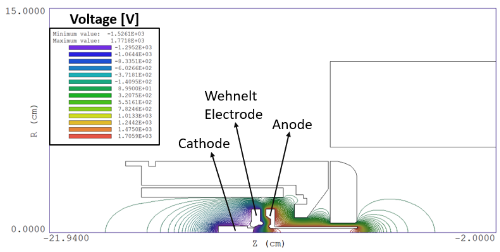

Figure 5: Electrostatic field map using potentials $V_C = -1500$, $V_W = -1510$, and $V_A = +1753.4$ V respectively.

TRAK simulation may also incorporate an independently applied magnetic field solution. The solution is computed on a separate mesh and adapted to the geometry of magnetic components (i.e the two flat coils and the ARMCO iron shielding). The bucking coil is turned off for all simulations. Figure 6 shows the combined axial magnetic field from the two flat coils using the parameters from Table 1. Convergence was obtained by scanning different solution

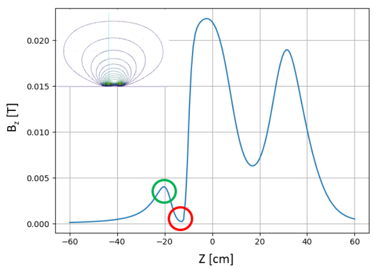

Figure 6: Combined axial magnetic field from two flat coils. Circled in red the magnetic field at the cathode (0.0002T), in green the peak from the magnetised iron shielding. Insert: closed contour lines for converged solution.

volumes while applying Dirichlet boundary conditions. The theoretical on-axis magnetic field at the coil midplane for a coil with finite length and radial thickness is given by [12]:

$$\mathbf{B} = \frac{\mu_0 N i}{2\,(r_2 - r_1)} \ln \left[\frac{\sqrt{r_2^2 + (l/2)^2} + r_2}{\sqrt{r_1^2 + (l/2)^2} + r_1} \right] \tag{2}$$

(where Ni represents the current-turns and r_i and L are the radial and longitudinal extents of the coil, respectively). The TRAK solution differs to the theoretical value by 0.001%.

PARTICLE TRACKING

TRAK computes trajectories of charged particles in specified electric and magnetic fields, including space-charge effects via self-consistent field updates at each time step. Model particles are emitted from a defined surface according to the CL law[2], with a generation surface offset from the emission boundary. Convergence was evaluated based on minimum and stable number of cycles needed to recompute the space charge, achievement of the target residual (average error in the electrostatic potential), and convergence of the beam current. All three conditions were satisfied. The particle trajectories in TRAK are also computed with 2D ray tracing code IGUN using the same initial conditions (via CL law) and electric field recalculation parameters (over-relaxation, number of iteration cycles, etc.). To include the magnetic field from TRAK, the field data was imported into IGUN. Figure 7 illustrates the results. Both IGUN and TRAK show

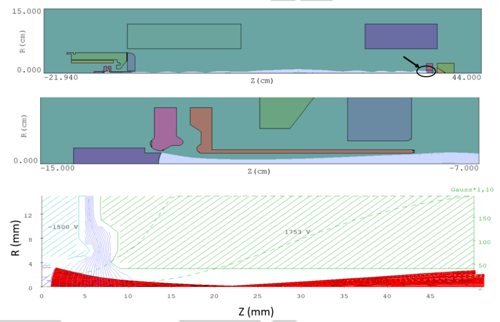

Figure 7: Upper: TRAK trajectories (white) from cathode to Faraday Cup aperture (circled black). Middle: TRAK zoom-in of the gun region. Lower: IGUN trajectories in red. Magnetic field represented as dotted green line (units in Gauss).

similar electron trajectories. Electrons are initially focused by the electric field and after exiting the anode, are guided and adiabatically compressed by the magnetic field from the two flat coils ($j \propto B_z^2$) until they reach the Faraday Cup. Under Brillouin flow conditions, the space-charge forces are exactly compensated by the magnetic forces, leading to the beam reaching its maximum achievable compression. Further studies are nevertheless required to quantitatively assess the agreement between the two codes, particularly in terms of electron phase space evolution along the beamline.

CONCLUSION

In this paper, realistic finite element simulations are used to assess the feasibility of a proposed test-stand for the new CANREB electron gun. A dedicated TRAK model shows that key requirements are met, including proper electron emission, beam compression by magnetic flat coils, and efficient collection at the Faraday cup. Further studies are needed to evaluate the thermal limits of the flat coils, as higher magnetic fields are required for stronger compression of higher electron currents for ion trapping.

[2] Current and kinetic energy are thus based on the preset values of the electric field.

REFERENCES

[1] S. Saminathan *et al.*, "Design of a multi-harmonic buncher for triumf 500 mev cyclotron", in *Proc. Cyclotrons'22*, Dec. 2022. doi:10.18429/JACoW-CYCLOTRONS2022-TUAO04

[2] B. E. Schultz, C. R. J. Charles, M. Cavenaile, R. Kanungo, F. Ames, and O. Kester, "Canreb ebis commissioning at triumf", *Journal of Physics: Conference Series*, vol. 2244, no. 1, p. 012028, 2022. doi:10.1088/1742-6596/2244/1/012028

[3] J. A. Bagger *et al.*, "ARIEL at TRIUMF: science and technology", in *Proc. 9th Int. Particle Accelerator Conf. (IPAC'18)*, pp. 6–11, Apr. 2018. doi:10.18429/JACoW-IPAC2018-MOXGB2

[4] B. E. Schultz, M. Cavenaile, M. Hartmann, F. Ames, and O. Kester, "CANREB developments at TRIUMF", in *Proc. 21st International Conference on Ion Sources (ICIS'25)*, Sep. 2025.

[5] Field Precision LLC, Trak charged particle toolkit 8.0, 2024, https://www.fieldp.com/trak.html

[6] R. Becker and W. B. Hermannsfeldt, "IGUN–A program for the simulation of positive ion extraction including magnetic fields", *Review of Scientific Instruments*, vol. 63, no. 4, p. 2756, 1992.

[7] L. Brillouin, "A theorem of larmor and its importance for electrons in magnetic fields", *Physical Review*, vol. 67, pp. 260–266, 1945. doi:10.1103/PhysRev.67.260

[8] J. D. Cardona *et al.*, "Simulations of a new electron gun for the TITAN EBIT", *Journal of Physics: Conference Series*, vol. 2244, p. 012075, 2022. doi:10.1088/1742-6596/2244/012075

[9] A. Laxdal *et al.*, "High power allison scanner for electrons", in *Proc. BIW2012*, 2012. https://api.semanticscholar.org/CorpusID:110648421

[10] L.-T. Yeh, "Thermal design guide of liquid cooled systems", in in *Thermal design of liquid cooled microelectronic equipment*, ed. by L.-T. Yeh, ASME Press, 2019,

[11] C. D. Child, "Discharge from hot CaO", *Phys. Rev. (Series I)*, vol. 32, pp. 492–511, 1911. doi:10.1103/PhysRevSeriesI.32.492

[12] NetDenizen, Emagnet, n.d. https://netdenizen.org/emagnet/